ELSEVIER

Thermochimica Acta 298 (1997) 9–16

thermochimica acta

The influence of heat transfer on temperature-modulated DSC measurements

J.E.K. Schawe*, W. Winter

Universität Ulm, Sektion für Kalorimetrie, D-89069 Ulm, Germany

Received 28 November 1996; received in revised form 14 March 1997; accepted 4 April 1997

Abstract

The calibration functions of amplitude and phase lag of the dynamic heat-flow rate of temperature-modulated DSC are investigated by model calculations. The results are experimentally verified for sapphire and polystyrene. The calibration functions depend on the sample as well as the heat-transport conditions on the sample holder. At low frequencies, these functions are constant. However, for calibration in the entire frequency range, the knowledge of these functions is necessary. The frequency dependence of phase lag and amplitude are investigated. The calibration functions are determined by the actual heat-transfer parameter. Using the presented model, this parameter can be evaluated from phase-lag information and can be used for the amplitude calibration. © 1997 Elsevier Science B.V.

Keywords: Calibration; Linearity; Temperature-modulated differential scanning calorimetry (TM-DSC)

1. Introduction

The temperature-modulated DSC (TM-DSC) is an extension of the conventional DSC. At this measuring mode, the conventional temperature program (isothermal and linear scan) is superimposed with a periodic change.

$$T(t) = T_0 + \beta_0 t + T_a \sum_{n=1}^{\infty} a_n \sin(n\omega_0 t) \qquad (1)$$

where T_0 is the initial temperature, β_0 the constant underlying scanning rate, T_a the temperature amplitude of the periodic component, $\omega_0 \equiv 2\pi f = 2\pi/t_p$ (f is the frequency of the periodic component and t_p the period) and a_n a set of parameters (Fourier coefficients), which describes the shape of the periodic signal. In the linear case, it was shown that the sample signal Φ_s can be described as a sum of an underlying component Φ_u and a periodic component Φ_p. [1,2].

$$\Phi_s = \Phi_u + \Phi_p \qquad (2)$$

The underlying component is equivalent to the conventional DSC curve. The periodic component is

$$\begin{aligned}\Phi_s(t,T) &= \Phi_a(\omega_0,T)\sum_{n=1}^{\infty} a_n \cos(n\omega_0 t - \varphi_n) \\ &\equiv \omega_0 T_a |C(\omega_0,T)| \sum_{n=1}^{\infty} a_n \cos(n\omega_0 t - \varphi_n) \\ &= \omega_0 T_a \sum_{i=1}^{\infty} a_n (C'(n\omega_0,T)\cos n\omega_0 t \\ &\quad + C''(n\omega_0,T)\sin n\omega_0 t) \end{aligned} \qquad (3)$$

where φ is the phase lag between the heat-flow rate and the temperature change and Φ_a the amplitude of the heat-flow rate. C' is the real part and C'' the

*Corresponding author. Fax: 00 49 731 502 3112.

PII S0040-6031(97)00161-5

imaginary part of the complex heat capacity

$$C(\omega) = C'(\omega) - iC''(\omega) \tag{4}$$

The modulus of the heat capacity is

$$|C(\omega)| = \sqrt{C'(\omega)^2 + C''(\omega)^2} \tag{5}$$

The influence of heat transfer on the measured signal (smearing) was considered but not discussed in an earlier paper ([2]). We want to discuss these effects in detail here.

2. The influence of the DSC on the measured curves

A DSC can be described as a linear system within the limits of accuracy of the measurements. The connection between the sample signal Φ_s and the measured signal Φ_m is given by the convolution product

$$\Phi_m(t) = \int_0^t G(t-t')\Phi_s(t')\mathrm{d}t' \tag{6}$$

The Green's function (or impulse response function) G describes the influence of the measuring device on the measured curve. Substituting Eq. (2) in Eq. (6) yields

$$\Phi_m(t,T) = \int_0^t G(t-t')\Phi_u(t',T)\mathrm{d}t' + \int_0^t G(t-t')\Phi_p(t',T)\mathrm{d}t' \tag{7}$$

The first term in this equation is equivalent to the smeared signal of a conventional DSC. The influence of G on the measured signal is discussed in Refs. [3,4]. A typical Green's function for a DSC (Perkin–Elmer DSC 2 and 18.41 mg polystyrene) is shown in Fig. 1. The maximum of G is at ≈10 s. After 30 s this function disappears. Because ω corresponds to the period t_p, an influence of the DSC on the measured curve is expected at periods lower then 30 s. At periods lower then 10 s, a strong smearing of the measured curve is expected. The lower limit of the period t_p should be close to the maximum time in G.

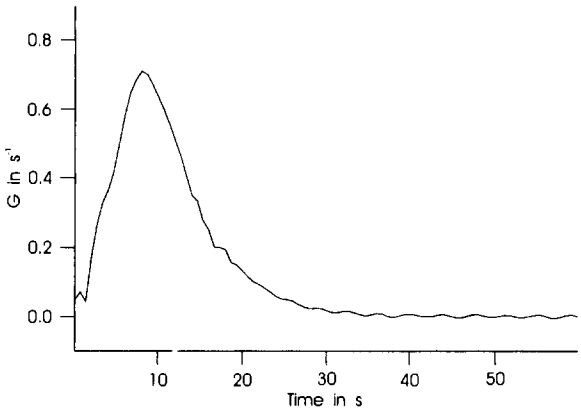

Fig. 1. Green's function of a Perkin–Elmer DSC-2 containing a 18.41 mg polystyrene sample.

For the following investigations only the second term of Eq. (7) is of interest. This term is equivalent to the measured curve at quasi-isothermal conditions. For a better understanding, the following calculations are based on a sinusoidal, periodic temperature change. The result can be generalized to any signal form by using Eq. (1).

$$T(t) = T_0 + T_a \sin(\omega_0 t) \tag{8}$$

In this case, the sample signal Φ_s is identical to Φ_p in Eq. (2). The measured signal reads

$$\Phi_m(t) = \int_0^t \Phi_s(t-t')G(t')\mathrm{d}t \tag{9}$$

It is useful to solve this equation by Fourier transformation

$$\mathcal{F}(\Phi_m(t)) \equiv \Phi_m(\omega) = \int_0^\infty \Phi_m(t)\exp(-i\omega t)\mathrm{d}\omega$$
$$\mathcal{F}^{-1}(\Phi_m(\omega)) \equiv \Phi_m(t) = \tfrac{1}{2\pi}\int_0^\infty \Phi_m(\omega)\exp(i\omega t)\mathrm{d}t \tag{10}$$

because the convolution product transforms to a conventional product

$$\Phi_m(\omega) = \phi_p(\omega)G(\omega) \tag{11}$$

The Green's function $G(t)$ is a real function and the Fourier transform $G(\omega)$ is complex

$$G(\omega) = G'(\omega) + iG''(\omega) \tag{12}$$

The Fourier transform of Φ_p (Eq. (3)) is

$$\Phi_p(\omega) = \omega_0 T_a(C'\pi\delta(\omega - \omega_0) - iC''\pi\delta(\omega - \omega_0)) \tag{13}$$

where $\delta(x)$ is the Dirac function. Finally, $\Phi_m(\omega)$ can be written as

$$\Phi_m(\omega) = \omega_0 T_a((C'G' + C''G'')\pi\delta(\omega - \omega_0) - i(C''G' - C'G'')\pi\delta(\omega - \omega_0)) \tag{14}$$

We obtain, for the measured signal, by inverse Fourier transformation of Eq. (14)

$$\begin{aligned}\Phi_m(t) &= \omega_0 T_a(G'(C'\cos\omega_0 t + C''\sin\omega_0 t) \\ &\quad + G''(C''\cos\omega_0 t)) \\ &\equiv \omega_0 T_a|C||G|\cos(\omega_0 t - \varphi - \varphi_g)\end{aligned} \tag{15}$$

A comparison of the measured signal $\Phi_m(t)$ (Eq. (15)) and the unsmeared sample signal $\Phi_s(t)$ (Eq. (3)) shows, that the heat transfer influences the amplitude for a factor $|G|$ and results in an additional phase lag φ_g. Both quantities depend on the measuring frequency. To calculate the sample parameters (i.e. the complex heat capacity ($C(\omega_0)$), it is necessary to determine this calibration functions.

Calculations of special heat-transfer models of the calorimeter yield similar results [5,6].

3. Model calculations for the calibration functions

A result of the previous paragraph is that the DSC influences the amplitude and phase lag of the measured signal. To obtain quantitative values and to find out their frequency dependences, model calculations are helpful. A simple model of the DSC sample holder is used (Fig. 2), with two identical furnaces. The temperature of the sensor is controlled. The samples should be infinitely thin. The real heat-flow rate into the sample is φ_s. The heat-flow rate φ_m is measured at the sensor location. The whole heat-transfer path into the furnaces, the heat contact and the heat transfer into the sample, is approached as one-dimensional heat conductor with the length L, the cross section A_c and the heat capacity C_f.. The sensor is located at $l = 0$ (on the bottom) and the sample at $l = L$ (on the top). The whole heat transfer path is described by the heat-

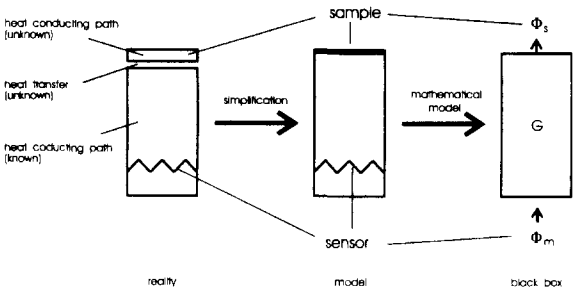

Fig. 2. Model of one DSC furnace with sample. The sample is approximated to be an infinitely thin foil. The heat-flow rate into the sample is Φ_s The Green's function G describe the heat transfer from the heater to the sample. The whole system is adiabatically isolated.

transfer coefficient

$$k = \frac{L}{A_c\lambda}C_f + k_t \tag{16}$$

where λ is the heat conductivity of the furnace material and k_t describes the heat conductivity of the sample and the heat contact; k_t depends on the heat capacity of the sample. This is a simple model of the sample holder of a power compensated DSC.

If the temperature change measured in location of the sensor is sinusoidal, then the heat-flow rate into the sample $\Phi_0(t)$ reads

$$\Phi_0(t) = \Phi_a\cos\omega_0 t \tag{17}$$

where the amplitude is

$$\Phi_a(t) = C_s\omega_0 T_a(L) \tag{18}$$

(C_s is the heat capacity of the sample and $T_a(L)$ the temperature amplitude on the top of the heat conductor.)

The heat-transfer coefficient k contains the heat-transfer conditions of the sample. Therefore, Φ_s is the heat-flow rate into the sample after correction of the heat transfer influence (desmearing) and consequently Φ_s is in phase with the temperature change on the place $l = L$. The solution of the field equation

$$\frac{\partial^2 T(z,t)}{\partial z^2} = \frac{k}{L^2}\frac{\partial T(z,T)}{\partial t} \tag{19}$$

yields the measured signal of the sensor. A useful method to obtain a solution of this linear partial differential equation is by means of the Laplace

transformation

$$T(s) = \int_0^\infty T(t)\mathrm{e}^{-st}\mathrm{d}t \tag{20}$$

where s is a complex value $s = \sigma + i\omega$.

In analogy to the calculations in [7], we obtain the temperature profile

$$T(s,z) = \frac{T_0}{s}\left(T(s,0) - \frac{T_0}{s}\right)\frac{\cosh\sqrt{ks}\frac{L-z}{L}}{\cosh\sqrt{ks}} - \frac{L\sinh\sqrt{ks}\frac{z}{L}}{\lambda A_c\sqrt{ks}\cosh\sqrt{ks}}\Phi_s(s) \tag{21}$$

where T_0 is the initial temperature and $T(s,0)$ the temperature at the location of the sensor.

The measured signal Φ_m is obtained by means of the Fourier law

$$\Phi_m(s) \equiv \Phi(z=0,s) = -\lambda A_c\frac{\partial T(z=0,s)}{\partial z} \tag{22}$$

This results in:

$$\Phi_m(s) = -\left(T(s,0) - \frac{T_0}{s}\right)\sqrt{ks}\frac{\lambda A_c}{L}\tanh\sqrt{ks} + \frac{1}{\cosh\sqrt{ks}}\Phi_s(s) \tag{23}$$

The first term in Eq. (23) does not depend on the sample. It describes the furnace. If the sample holders are symmetric, this term can be neglected. In this case the measured signal reads:

$$\Phi_m(s) = \frac{1}{\cosh\sqrt{ks}}\Phi_s = G(s)\Phi_s(s) \tag{24}$$

This relationship is a convolution product and $G(s)$ is the transforming Green's function. The back-transformation of Eq. (24) yields the convolution integral Eq. (9). The Green's function $G(t)$ is:

$$G(t) = \frac{\pi}{k}\sum_{n=0}^{\infty}(-1)^n(2n+1)\mathrm{e}^{-x_n t} \tag{25}$$

where

$$x_n = \frac{(2n+1)^2\pi^2}{4k}$$

Substitution of Eq. (17) into Eq. (9) yields

$$\Phi_m(t) = \Phi_a\frac{\pi}{k}\sum_{n=0}^{\infty}(-1)^n(2n+1) \times\left[\frac{1}{x_n^2+\omega_0^2}(x_n\cos(\omega_0 t) + \omega_0\sin(\omega_0 t))\frac{-x_n}{x_n^2+\omega_0^2}\mathrm{e}^{x_n t}\right] \tag{26}$$

If the exponential term vanishes one gets the steady state measured heat-flow rate:

$$\begin{aligned}\Phi_m(t) &= \Phi_a\frac{\pi}{4}\left(\cos(\omega_0 t)\sum_{n=0}^{\infty}(-1)^n(2n+1) \times\frac{x_n}{x_n^2+\omega_0^2} + \omega_0\sin(\omega_0 t)\sum_{n=0}^{\infty}(-1)^n \times(2n+1)\frac{1}{x_n^2+\omega_0^2}\right) = \Phi_a\frac{4}{k} \\ &\times\left(\cos(\omega_0 t)\sum_{n=0}^{\infty}(-1)^n\frac{(2n+1)^3}{(2n+1)^4+\alpha^2} + \alpha\sin(\omega_0 t)\sum_{n=0}^{t}(-1)^n\frac{2n+1}{(2n+1)^4+\alpha^2}\right) \\ &= \Phi_a(A\cos\omega_0 t + B\sin\omega_0 t) \\ &= K_a\Phi_a\cos(\omega_0 t - \varphi_g)\end{aligned} \tag{27}$$

where

$$\alpha = \frac{4\omega_0 k}{\pi^2} \tag{28}$$

$$A = \frac{4}{\pi}\sum_{n=0}^{\infty}(-1)^n\frac{(2n+1)^3}{(2n+1)^4+\alpha^2} \tag{29}$$

and

$$B = \alpha\frac{4}{\pi}\sum_{n=0}^{\infty}(-1)^n\frac{2n+1}{(2n+1)^4+\alpha^2} \tag{30}$$

The functions A and B depend on the measuring frequency and the heat-transfer coefficient k. The sample as well as the heat contact between sample and furnace influence k.

The calibration factor of the amplitude K_a is:

$$K_a = \sqrt{A^2+B^2} \tag{31}$$

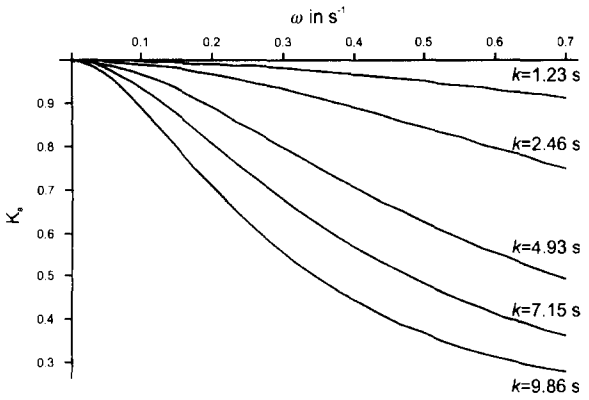

Fig. 3. The calculated calibration factor for the amplitude as a function of the frequency at different heat transfer coefficients.

The heat transfer yields the phase lag φ_g:

$$\varphi_g = \arctan \frac{B}{A} \tag{32}$$

The calibration functions of the heat-flow amplitude $K_a(k,\omega)$ and phase lag $\varphi_g(k,\omega)$ are functions of the frequency. K_a corresponds to $|C|$ in Eq. (15). In case of the heat flux DSC, the frequency dependence of K_a is already investigated experimentally [8]. In Fig. 3, the theoretical functions of K_a from Eq. (32) are shown. From these functions, one gets the typical behaviour of the amplitude. On increasing the frequency, the amplitude decreases. This effect depends on the heat-transfer coefficient. The better the heat transfer from the heater into the sample, the smaller is the influence on the amplitude. In Fig. 4, the related dependences in case of the phase lag are shown. Increasing k yields an increase in the phase lag. At higher frequencies, the influence of the heat-transfer coefficient rises.

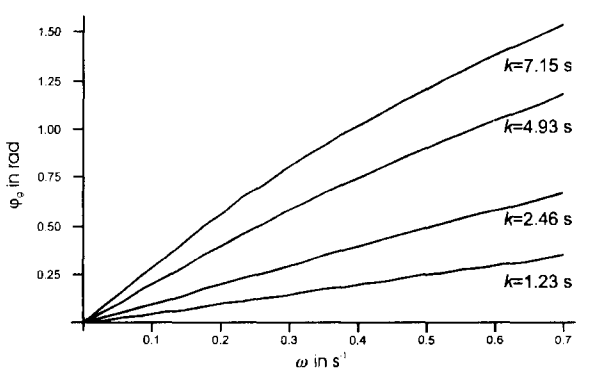

Fig. 4. The calculated phase lag as a function of the frequency at different heat-transfer coefficients.

4. Results

If the heat capacity C_p is known, and the sample has no thermal events, the calibration factor K_a can be calculated from the measured amplitude of the dynamic component Φ_{am}.

$$K_a(\omega_0) = \frac{\Phi_{am}(\omega_0, T)}{\omega_0 T_a(\omega_0) C_p(T)} \tag{33}$$

In this case the measured phase lag is identical with the phase calibration function φ_g.

The measuring device is a Perkin–Elmer DSC-7 in the DDSC mode. The average measuring temperature is 40°C. The program temperature amplitude is 1 K, unless otherwise stated. The heat-flow rate and the temperature are measured at varying frequencies in the (2–200) mHz range. The temperature amplitude and the amplitude of the heat-flow rate, as well as the phase lags are measured. The calibration function φ_g is obtained by subtracting φ_β from the measured phase lag φ_m. φ_β is determined from the behaviour of a real DSC sample holder (in contrast to the ideal symmetric sample holder describes by Eq. (24)). The calibration function of the heat-flow amplitude K_a is calculated by Eq. (33).

In order to determine the calibration function $\varphi_\beta(\omega)$, the measured amplitude calibration function $K_a(\omega)$ is fitted using Eq. (31). The result is the fit parameter k. The phase shift φ_g calculated from Eq. (32) is smaller than the measured phase shift φ_m. The difference between $\varphi_m(\omega)$ and $\varphi_g(\omega)$ is the instrument specific function φ_β.

The calibration functions are measured for different samples (sapphire samples of varying mass and thickness). The results are shown in Figs. 5 and 6. The samples differ in thickness and mass, so that the heat-transfer coefficient k varies. The experimental results correspond very well with the theoretical curves. This simple heat-transfer model is useful to describe the signal behaviour in this calorimeter in a wide frequency range. If ω_0 is less than 0.12 s^{-1} (period larger as 50 s) the calibration functions do not depend on the measuring conditions. Similar results are shown by comparison of sapphire and polystyrene (Figs. 7 and

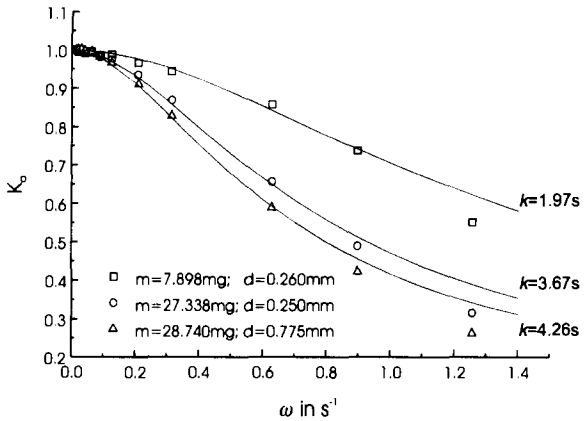

Fig. 5. The calibration factor for the heat-flow amplitude measured on sapphire samples of varying thickness and mass as a function of frequency. The black curves are theoretical curves (Eq. (31))

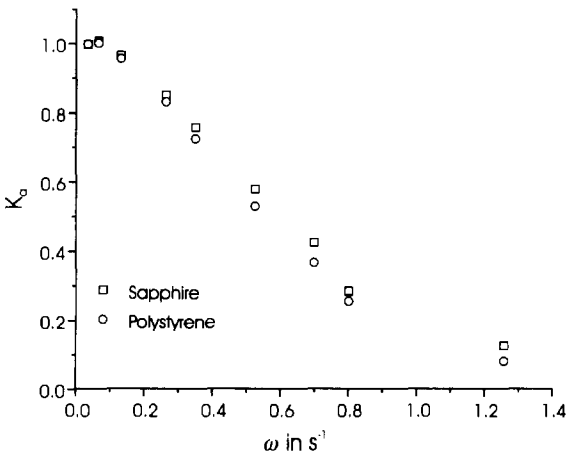

Fig. 7. The calibration factor of the heat flow amplitude of sapphire (27.338 mg) and polystyrene (18.342 mg).

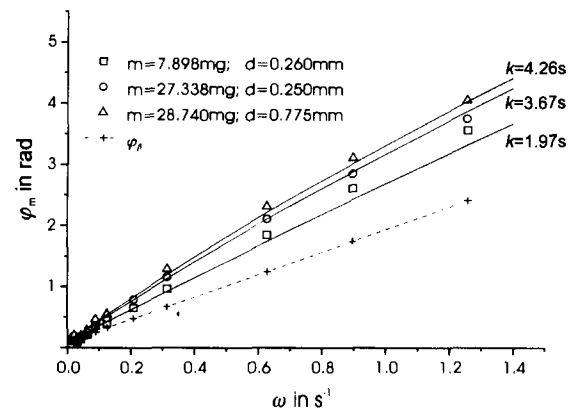

Fig. 6. The phase lag measured on sapphire samples of varying thickness and mass as a function of frequency. The black curves are theoretical curves (Eq. (32) and $\varphi_m = \varphi_g + \varphi_\beta$, where φ_β is the phase lag as determined by the behaviour of a real sample holder.).

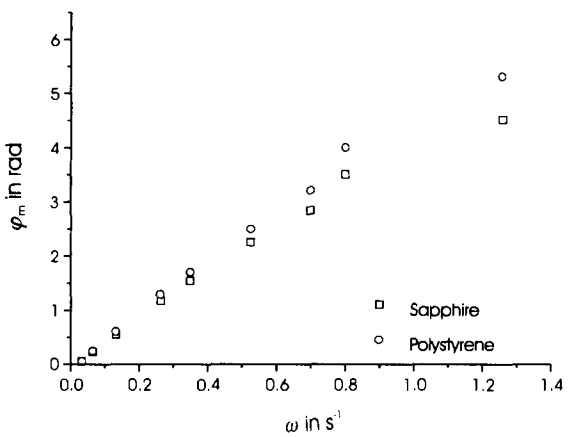

Fig. 8. The measured phase lag of sapphire (27.338 mg) and polystyrene (18.342 mg).

8). Especially in the high-frequency range (period less as 40 s), the heat-transfer conditions influence the calibration functions. In this region, the calibration should be carried out using substances with similar heat-transfer conditions as in the sample (e.g. polymer sample calibrated with polystyrene). The dependence of the calibration functions on the period t_p is shown in Figs. 9 and 10.

The model calculations show, that the calibration functions do not depend on the temperature amplitude (Eqs. (31) and (32)). For verification, the temperature amplitude is varied between 0.1 and 1 K. The sample is 8.652 mg polystyrene. The experimental results (Figs. 11 and 12.) show a good agreement with that of prediction. For higher frequencies ($\omega > 0.8\ s^{-1}$), the experimental errors increase and we obtain deviations between model calculations and experimental results.

5. Conclusion

The measured signal of TM-DSC measurements are influenced by heat-transfer conditions. The heat transfer into the DSC furnace, the heat transfer into the sample, and sample properties such as heat conduc-

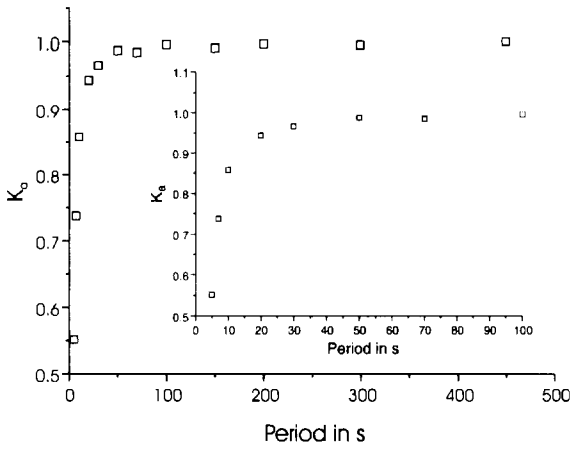

Fig. 9. The calibration factor of the heat-flow amplitude as a function of the period measured on sapphire (7.898 mg).

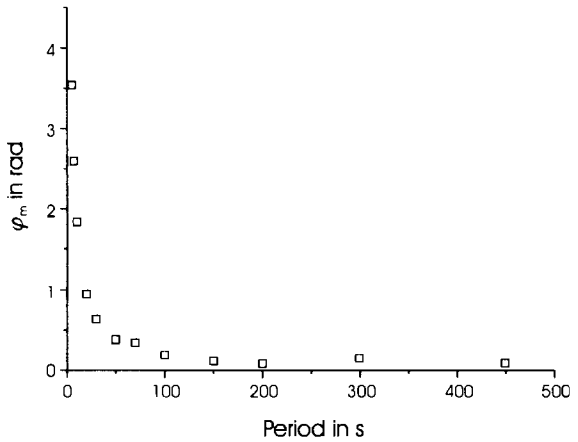

Fig. 10. The phase lag as a function of the period measured on sapphire (7.898 mg).

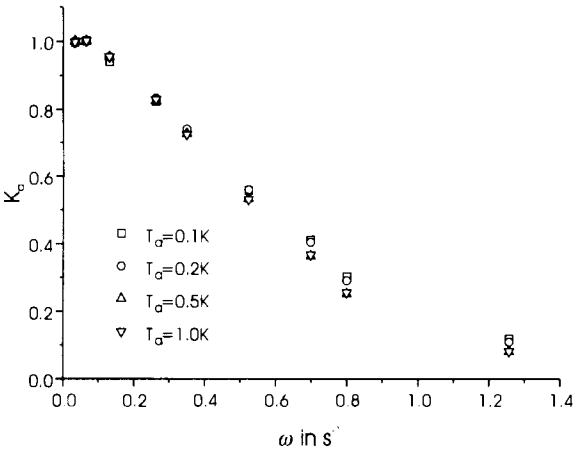

Fig. 11. The dependence of the heat-flow amplitude calibration function on the temperature amplitude (sample: 8.652 mg polystyrene).

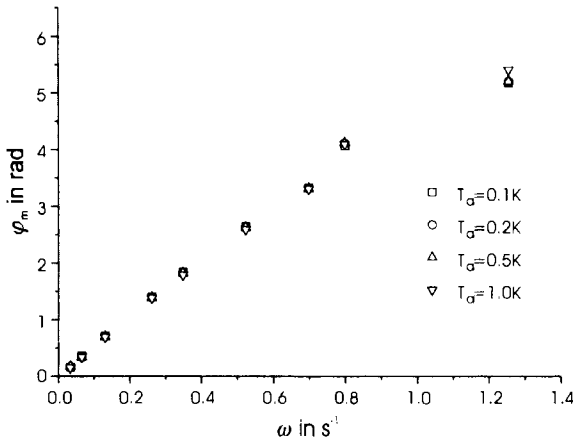

Fig. 12. The dependence of the measured phase-lag function on the temperature amplitude (sample: 8.652 mg polystyrene).

tivity and geometry affect the measured signal. It is advantageous to use relatively thin samples.

The measured signal is smeared by heat transfer. This smearing is the reason of the decrease in the heat-flow amplitude and the increase in the phase lag between heat-flow rate and temperature change. Without thermal event, the measured phase lag is the calibration function φ_g. These values can be used to calculate the phase lag of the sample in case of a thermal event. However during a real TM-DSC experiment, the heat capacity of the sample and the thermal contact can change. This influences the heat-transfer coefficient k. The change of the heat capacity can be considered in the calibration procedure. In addition, the heat contact between sample and pan should be good and relatively constant [9].

The calibration function of the amplitude depends on the frequency, the heat contact of the sample as well as on the geometry. In principle, it is possible to calibrate the amplitude within a large frequency range. In the low frequency range, this function is constant. The accuracy of heat capacity measurements at such conditions is better, and the calibration is nearly independent of the measurement conditions.

In the entire frequency range, the measured TM-DSC-signal can be described by the linear theory of

heat transfer. Substantial influences of the electronic controller on the signal shape are not measured.

References

[1] M. Reading, D.Elliott and V. Hill, 21st Proc. NATAS Conf., 1992, p.145-150.
[2] J.E.K. Schawe, Thermochim. Acta, 261 (1995) 183.
[3] G.W.H. Höhne and J.E.K. Schawe, Thermochim. Acta, 229 (1993) 27; J.E.K. Schawe, C. Schick and G.W.H. Höhne, Thermochim. Acta, 229 (1993) 37; J.E.K. Schawe, G.W.H. Höhne and C. Schick, Thermochim. Acta, 244 (1994) 33; J.E.K. Schawe, C. Schick and G.W.H. Höhne, Thermochim. Acta, 244 (1994) 49; J.E.K. Schawe, W. Winter and G.W.H. Höhne, submitted in Thermochim. Acta.
[4] K.R. Löblich, Thermochim. Acta, 83 (1985) 99, 263.
[5] J. Font Barrio, J. Muntassell and J.L. Tamarit, J. Thermal. Anal., 37 (1991) 39.
[6] B. Wunderlich, Y. Jin and A. Boller, Thermochim. Acta, 238 (1994) 277.
[7] H. Hoff, Thermochim. Acta, 187 (1991) 293.
[8] S.R. Sauerbrunn, P.S. Gill and J.A. Foreman, 23rd Proc. NATAS Conf., 1994, p. 51–56.
[9] J.E.K. Schawe, M. Margulies and B. Cassel, in preparation.